Lecture 5
H Saibil

Contrast transfer and CTF correction

The weak phase approximation
Contrast transfer function
Determining defocus
CTF correction methods

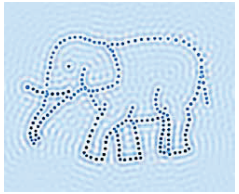

Image processing for cryo microscopy

5 - 15 September 2017

EMBO

Practical Course
Birkbeck College London

Contrast transfer

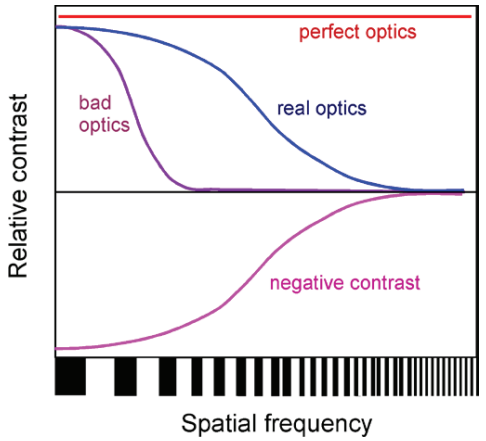

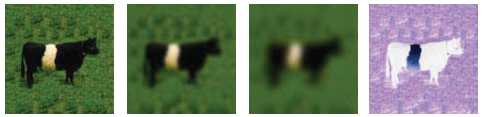

perfect optics | normal optics | bad optics | negative contrast

Why do we need to bother with defocus?

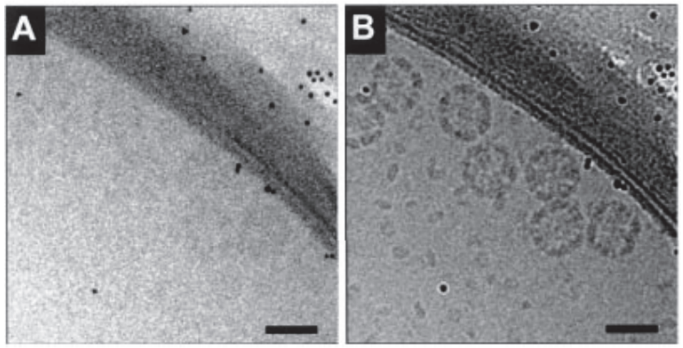

2 μm 7 μm

Tricorn protease, Walz, J et al (1997) Mol Cell 1, 59-65

The weak phase approximation

Review of Lecture 4:

EM image = projected electron scattering density of object modified by the CTF

If the object is thin and weakly scattering (ie made of light atoms), a simplified form of the CTF function can be derived.

The phase shift $\Phi(\mathbf{r})$ from a **weak phase object** is small, and the wave expression $\psi \exp[i\Phi(\mathbf{r})]$ can be approximated by the series

$$\psi\,[1 + i\Phi(\mathbf{r}) - \tfrac{1}{2}\,\Phi(\mathbf{r})^2 + 1/3\,\Phi(\mathbf{r})^3 - \ldots]$$

Because the phase shift is small, the 3rd order and higher terms can be ignored.

This approximation, combined with the phase shift introduction by **spherical aberration**, leads to the expression for the *phase contrast transfer function*, given on the next slide.

Phase CTF formula from the weak phase approximation

$$\text{Phase CTF} = -2 \sin [\pi(\Delta z \lambda q^2 - C_s \lambda^3 q^4/2)]$$

C_s – spherical aberration coefficient
ΔZ – defocus
q – spatial frequency
λ – electron wavelength

Ideal CTF curves

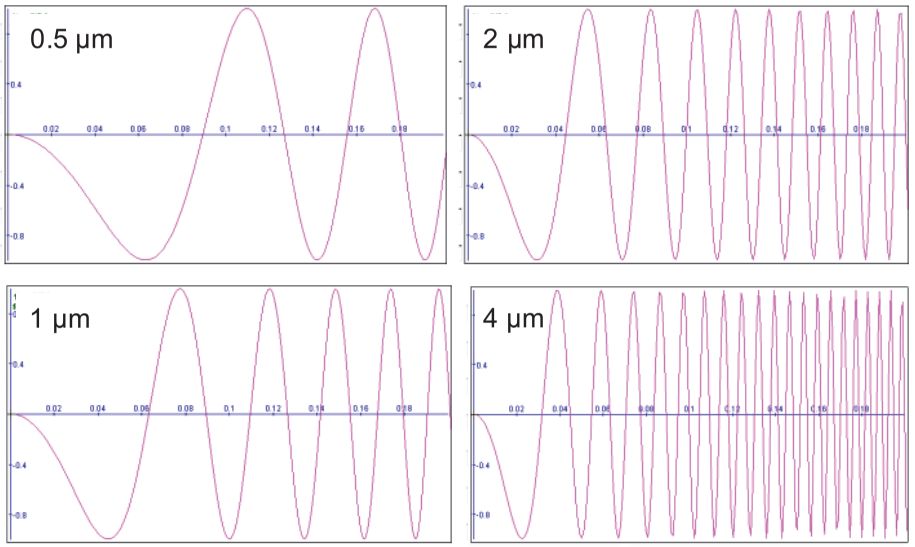

FEG images of carbon film

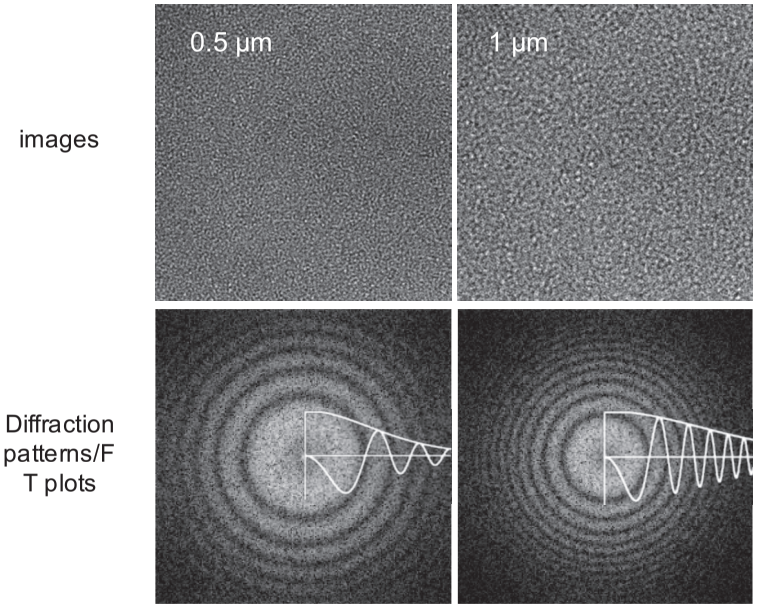

Causes of CTF decay

- Loss of spatial coherence - source size

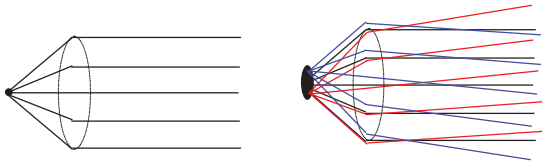

- Image drift
- Thick ice
- Specimen charging
- Chromatic aberration - variation in voltage
- Variation of lens current

Decay caused by loss of spatial coherence

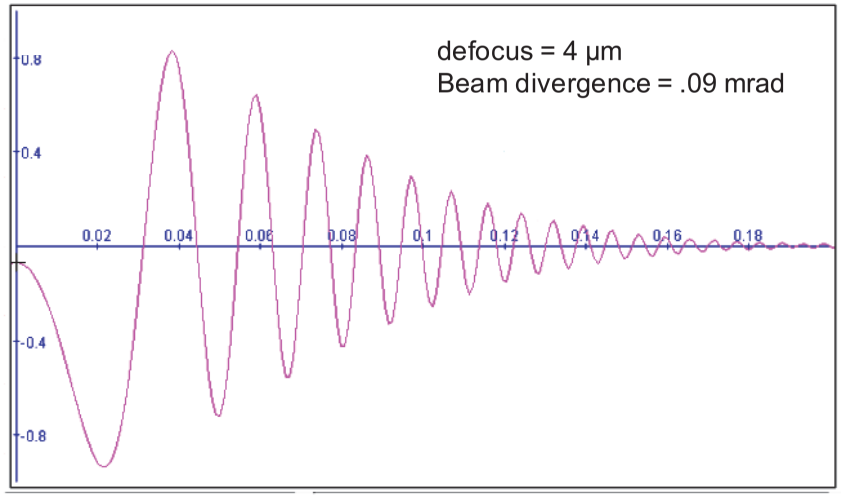

defocus = 0.5 - 4 µm
Beam divergence = 1 mrad

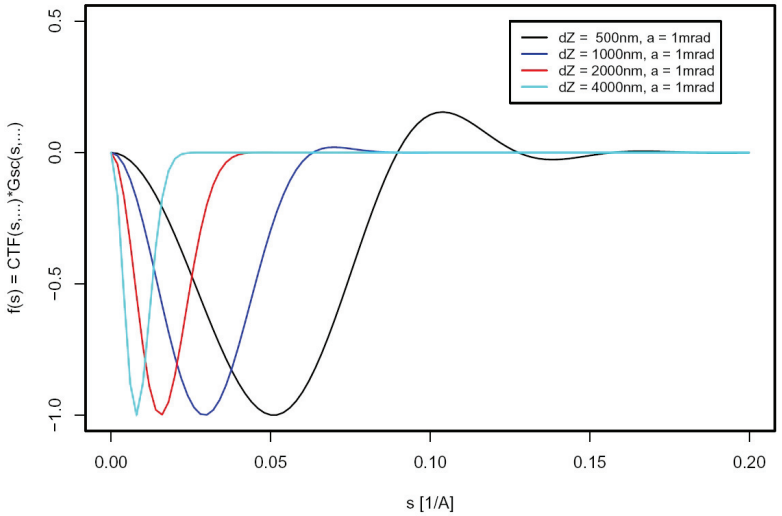

Drift and jumping

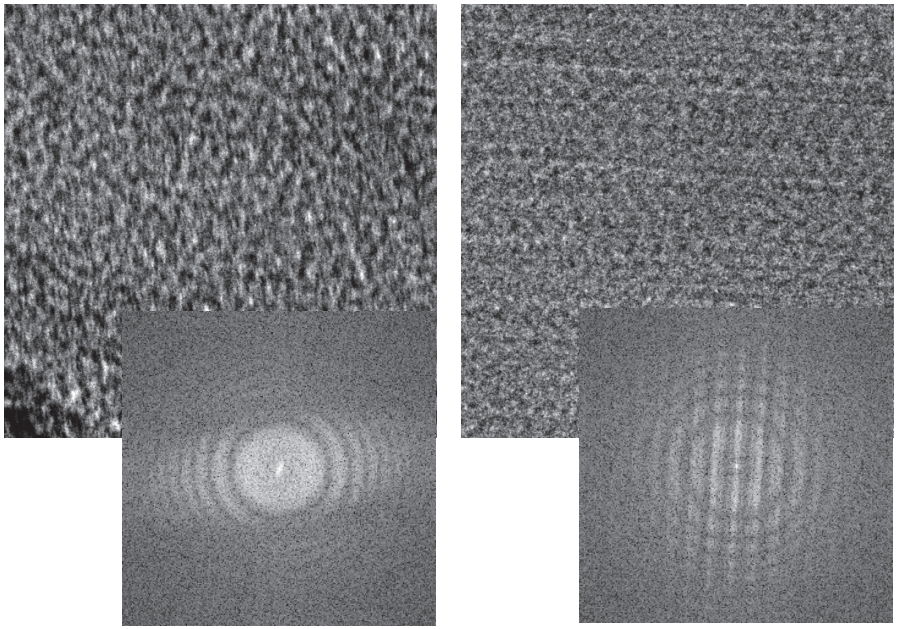

Effect of drift on the CTF

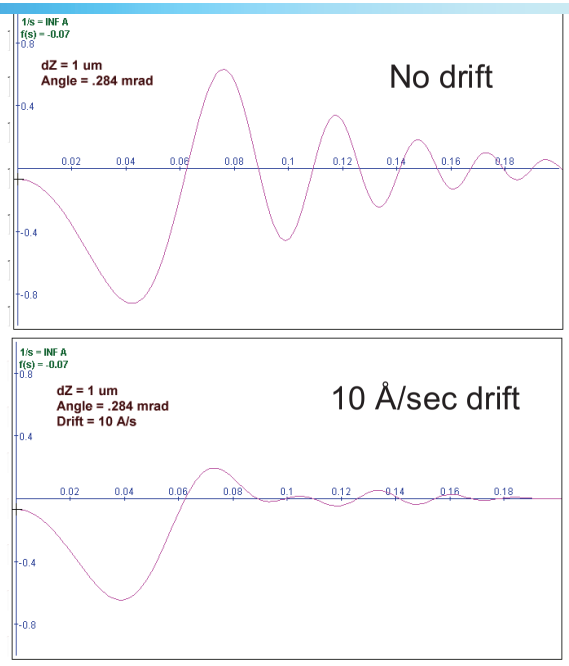

The CTF is the FT of the Point Spread Function

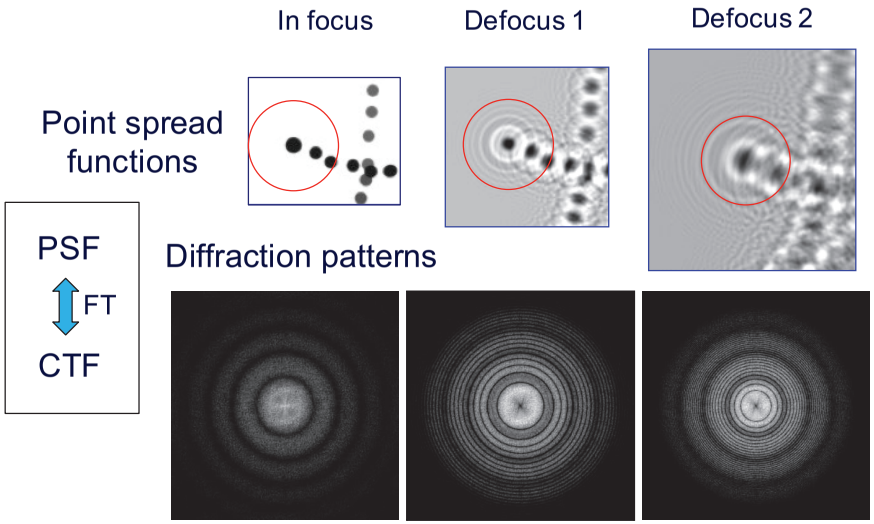

Effects of CTF on 2D projections

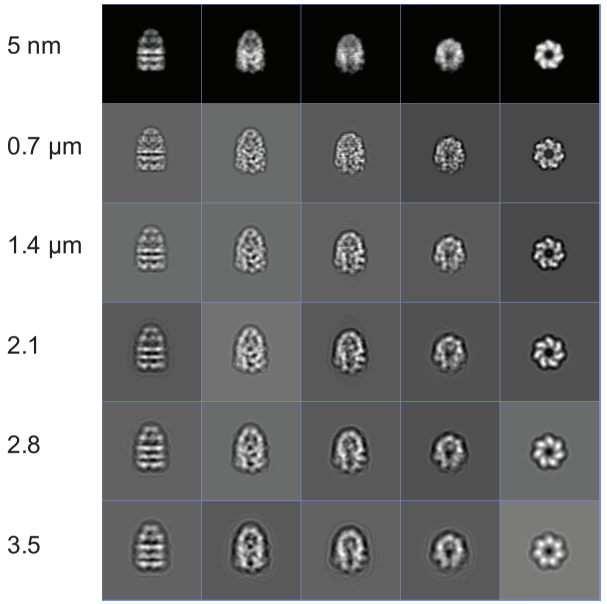

Effects of CTF on a 3D map

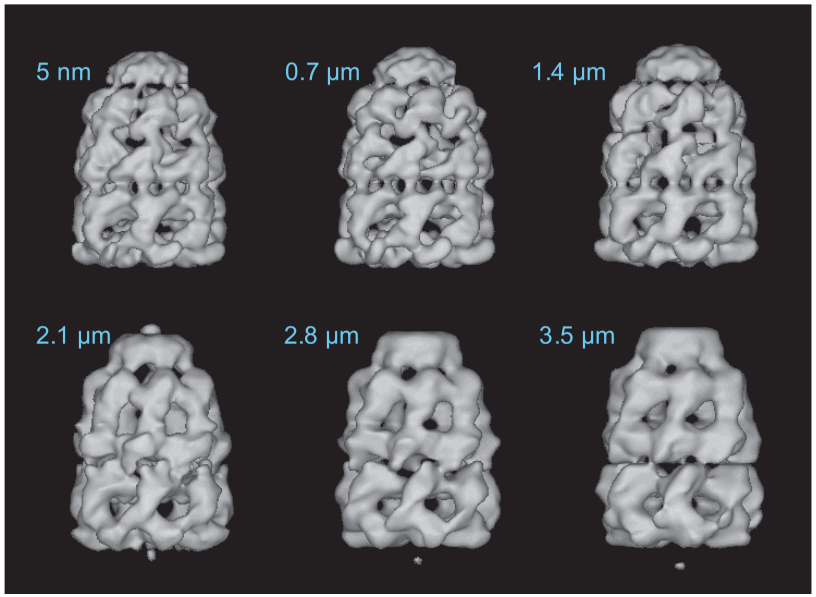

Tilt geometry and defocus

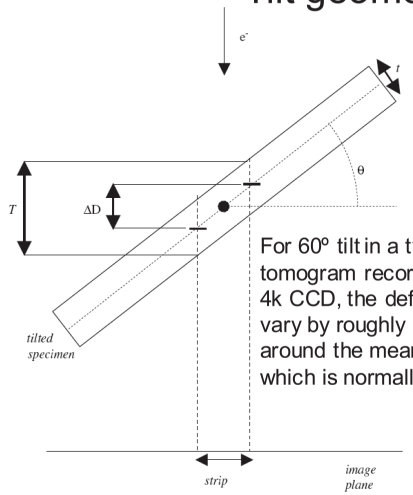

For 60° tilt in a typical tomogram recorded on a 4k CCD, the defocus will vary by roughly ±1 µm around the mean value, which is normally 4-15 µm.

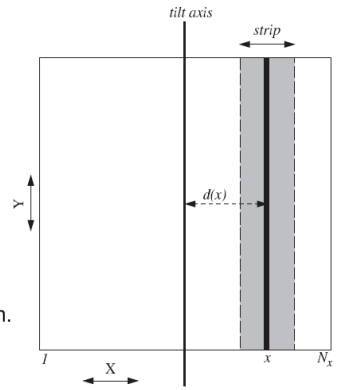

Fig. 1. Computation of a strip in an image of a tilted specimen. ΔD represents the defocus range considered as a single defocus value, T denotes the defocus range in the strip, t is the thickness of the specimen and θ is the tilt angle. The tilt axis runs perpendicular to the sheet and is marked by the black circle in the middle of the specimen slab.

Fig. 4. Extraction of a strip with a single effective defocus value from a tilted specimen. The square represents an image acquired from the tilted specimen. The tilt axis runs along the Y-axis. x denotes the index of the x-line around which the strip is extracted. $d(x)$ represents the distance from the x-line to the tilt axis.

from Fernandez, Li & Crowther (2006) CTF determination and correction in electron cryotomography. Ultramicrosc. 106, 587-596. Strip CTF correction is implemented in IMOD

Why don't I see Thon rings???

- Ice too thick
- No carbon in image
- Too little specimen – vitreous ice alone does not give Thon rings! (and too thin ice excludes sample)
- Too close to focus on a non-FEG source

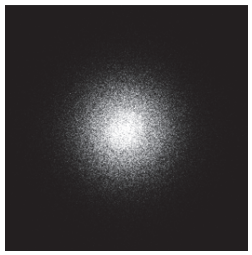

Measuring defocus

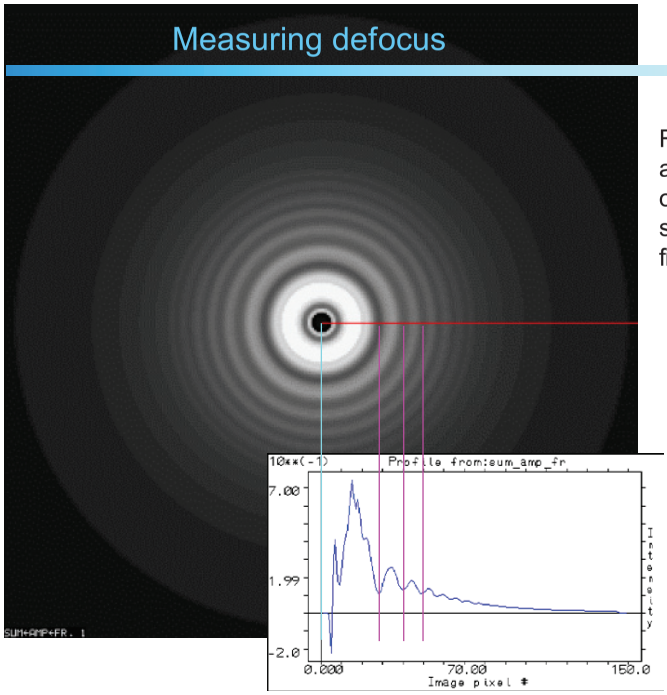

Rotationally averaged total sum of image power spectra; band-pass filtered

Profile of the averaged spectrum

CTF ripples are superposed on a large background of incoherent scattering, noise and other features

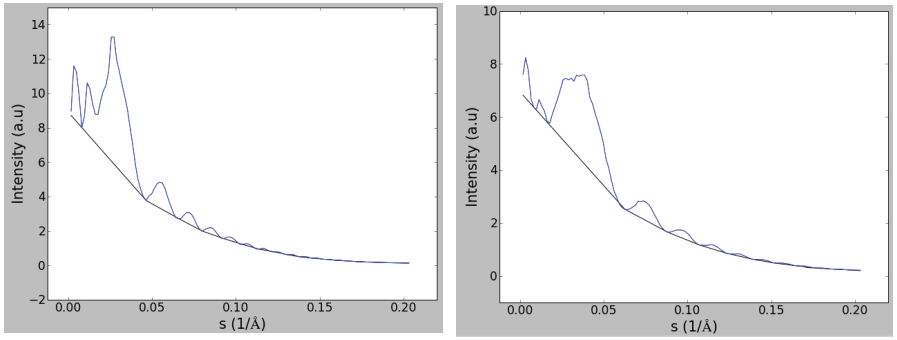

Background fitting and subtraction give a more accurate view of the CTF ripples

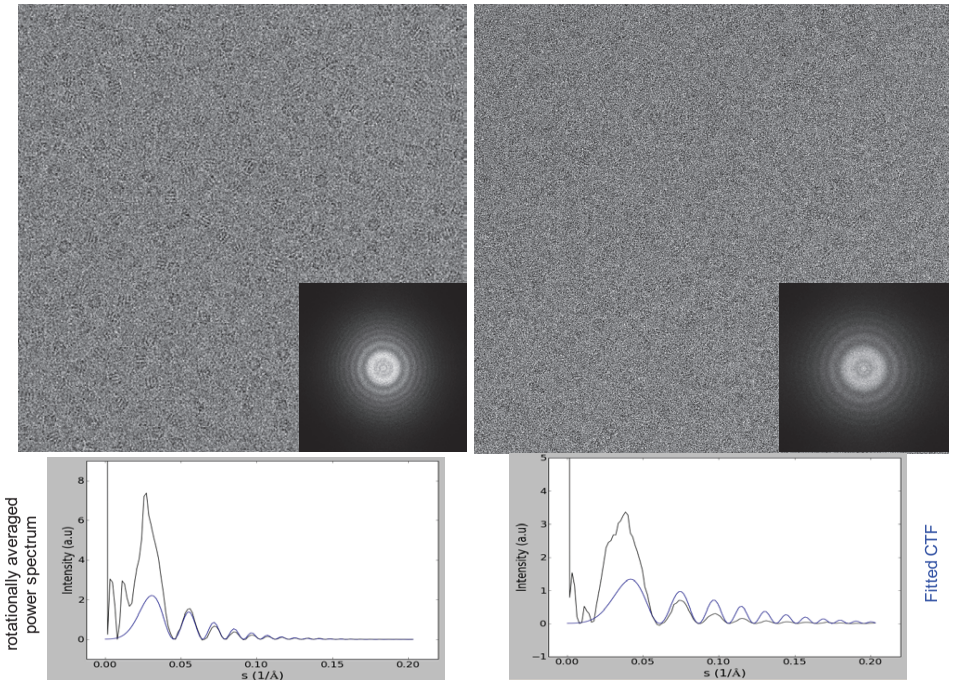

Procedures for measuring defocus

SPIDER/WEB - graphical interface for overlaying experimental and theoretical curves
http://spider.wadsworth.org/spider_doc/spider/docs/spider.html

EMAN2 - evalimage graphical interface
http://blake.bcm.edu/emanwiki/EMAN2/Programs/e2evalimage

CTFFIND4 – graphical/automated
Chops up areas into boxes
Uses estimate of starting defocus
Searches over a specified range of defocus
Estimates astigmatism
Gives split display output for verification of result
http://grigoriefflab.janelia.org/ctffind4

BSOFT graphical/automated
http://lsbr.niams.nih.gov/bsoft/

CTFFIND4 output

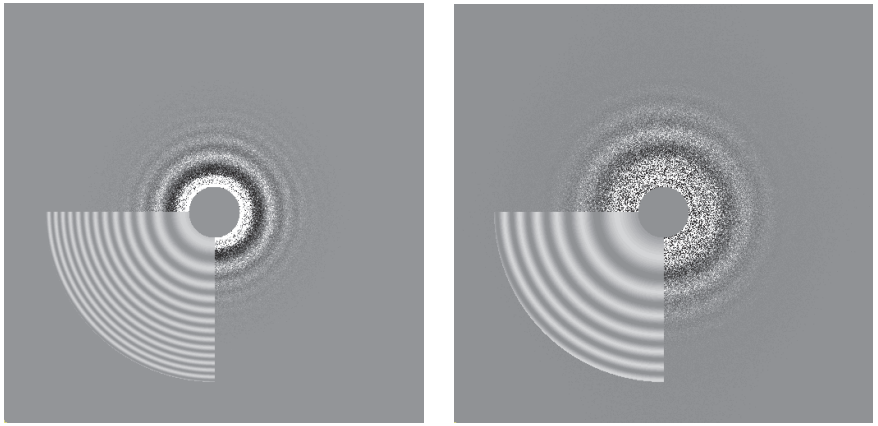

Defocus 2.405, 2.442 µm

Defocus 1.146, 1.219 µm

Astigmatism

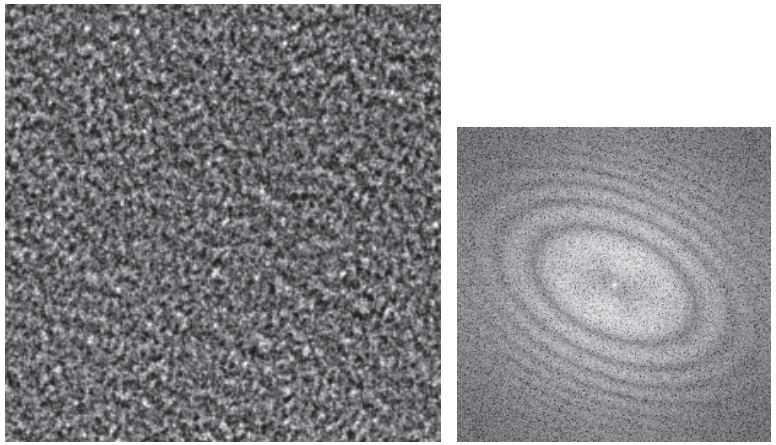

Astigmatic: defocus 1 = 4.41 µm, defocus 2 = 4.14 µm

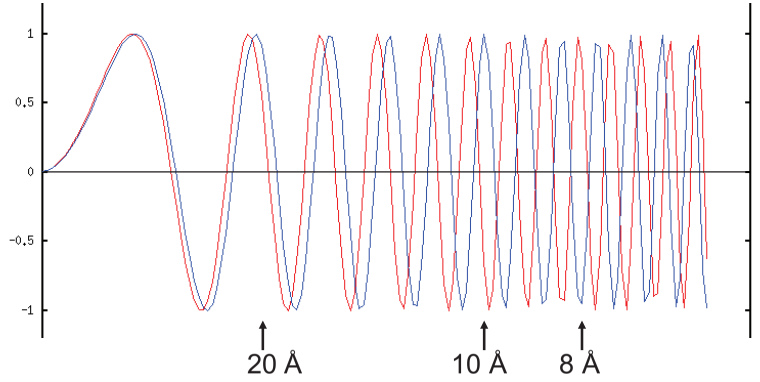

Astigmatic

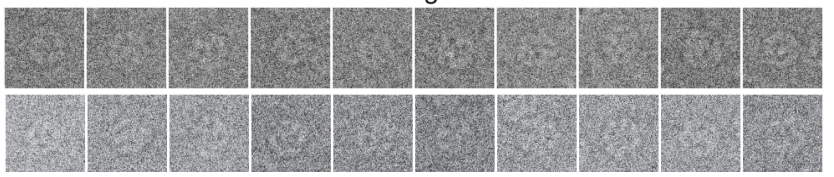

4 µm, no astigmatism

How to measure an astigmatic CTF

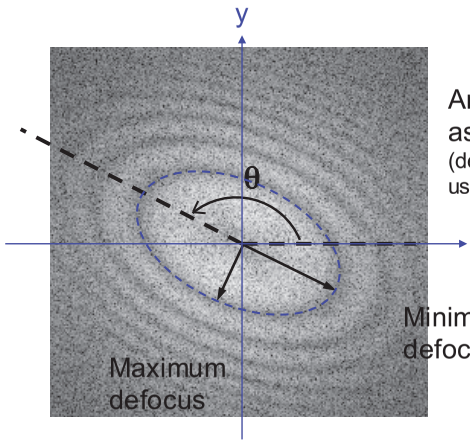

Angle of astigmatism, θ
(depends on convention used by your program)

The ellipse must be fitted or measured in sectors to get the degree and angle of astigmatism so that the zeroes can be correctly determined for all directions.

What range of defocus is needed?

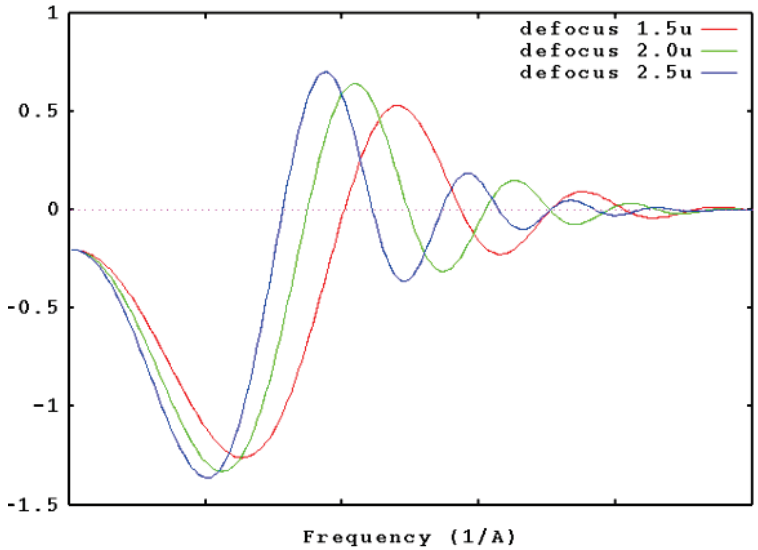

CTF curves from different images in a dataset

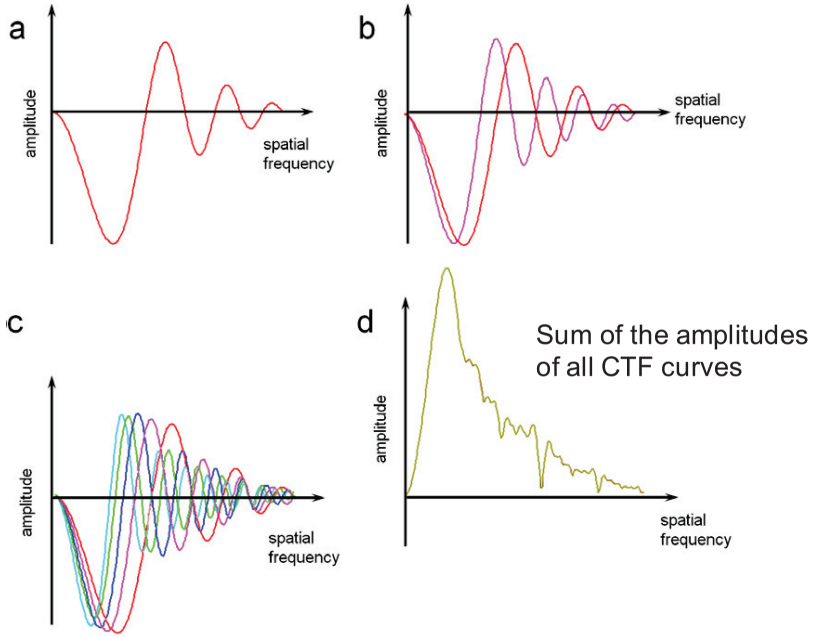

Methods of CTF correction

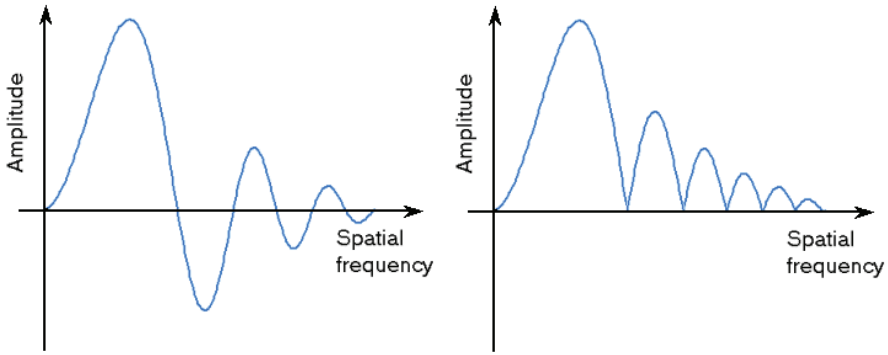

1. Phase flipping - can be done on raw images

2. Full restoration of amplitudes: Multiply each image FT by its own CTF, then add up all the equivalent views and divide the sum by the sum of all the CTF's squared, plus a constant related to the signal:noise ratio (Wiener factor) to avoid division by zero.

$$FT\_Merged\_class = \frac{\sum_{i=1,N} FTclass_i . CTF_i}{\sum_{i=1,N} (CTF_i^2) + w}$$

Effect of Wiener filtering

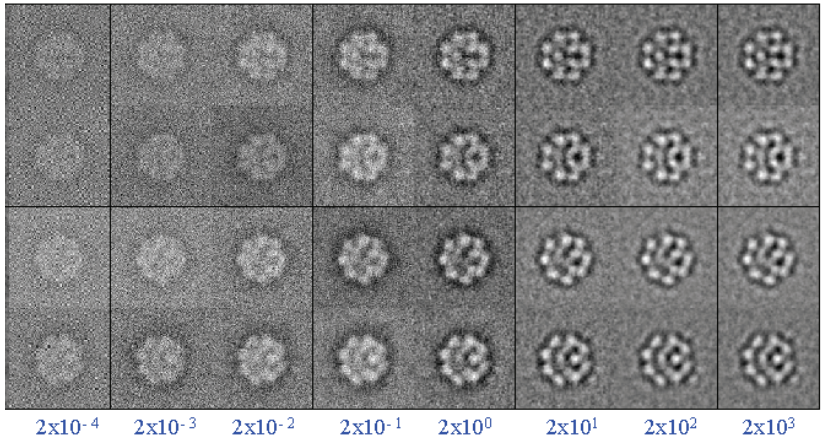

The larger the value of w, the more small fluctuations are suppressed - similar to low pass filtering

Steps in full amplitude restoration

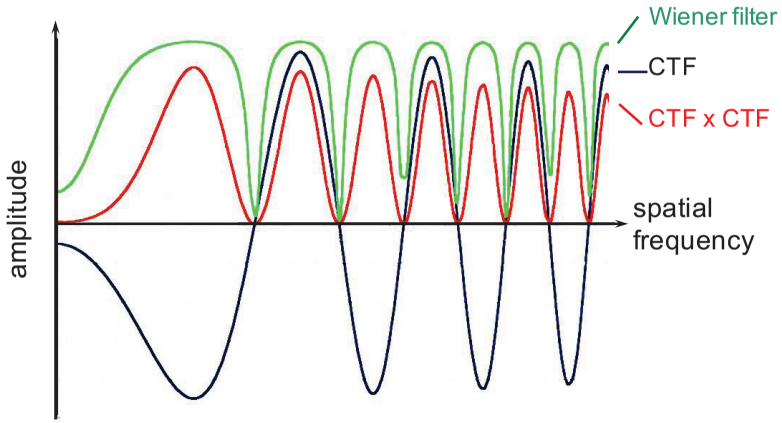

This can only be done by combining images of different defocus

Merging images of different defocus – model data

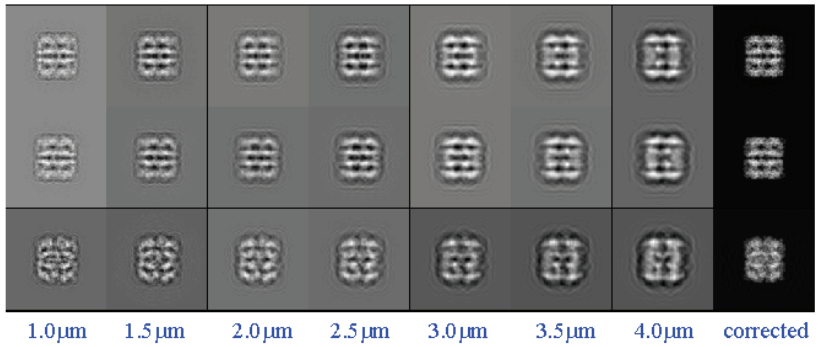

References

Frank, J (2006) Three-dimensional electron microscopy of macromolecular assemblies. Oxford University Press

Reimer, L (1989) Transmission electron microscopy. Springer-Verlag, Berlin

Hawkes & Valdrè (1990) Biophysical electron microscopy. Academic Press, London.

Toyoshima & Unwin (1988) Contrast transfer for frozen-hydrated specimens: determination from pairs of defocused images. Ultramicroscopy 25, 279-291.

Wade, R. H. (1992) A brief look at imaging and contrast transfer. Ultramicrosc. 46:145-156.

Toyoshima, C., K. Yonekura and H. Sasabe (1993) Contrast transfer for frozen-hydrated specimens II. Amplitude contrast at very low frequencies. Ultramicrosc. 48:165-176.

Erickson, H. P. and A. Klug (1971) Measurement and compensation of defocusing and aberrations by fourier processing of electron micrographs. Phil. Trans. R. Soc. Lond. B. 261:105-118.

Unwin, P. N. T. (1973) Phase contrast electron microscopy of biological materials. J. Microsc. 98:299-312.

Rohou, A & Grigorieff, N (2015) CTFFIND4: Fast and accurate defocus estimation from electron micrographs. J Struct Biol, *in press*.

Mallick SP, Carragher B, Potter CS, Kriegman DJ. (2005) ACE: automated CTF estimation. Ultramicroscopy 104, 8-29.

Winkler (2007) 3D reconstruction and processing of volumetric data in cryo-electron tomography. J. Struct. Biol. 157, 126-137.

Xiong Q, Morphew MK, Schwartz CL, Hoenger AH, Mastronarde DN (2009) CTF determination and correction for low dose tomographic tilt series. J. Struct. Biol. 168, 378-387.

Zanetti, Z, Riches, JD, Fuller, SD, Briggs, JAG (2009) Contrast transfer function correction applied to cryo-electron tomography and sub-tomogram averaging. J Struct Biol 165, 308-312.

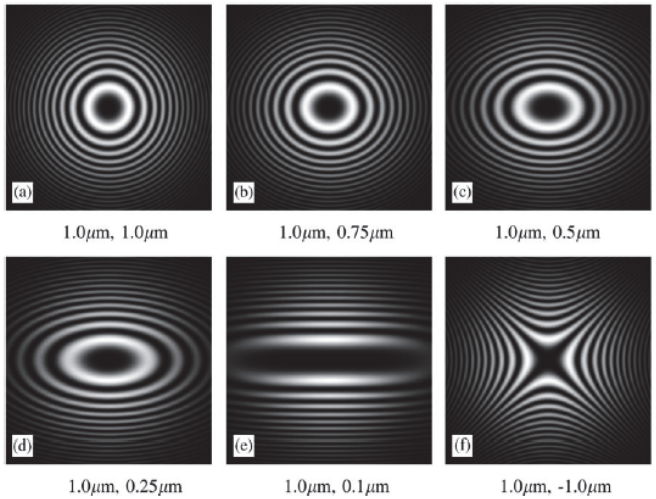

Fig. 1. Simulated power spectra with increasing astigmatism are shown. The caption shows the two defocus values corresponding to the power spectrum. The Thon rings can distort to an ellipse, a parabola or a hyperbola.

Comparison of the line profile of the rotationally averaged spectrum with the calculated contrast transfer function of the microscope

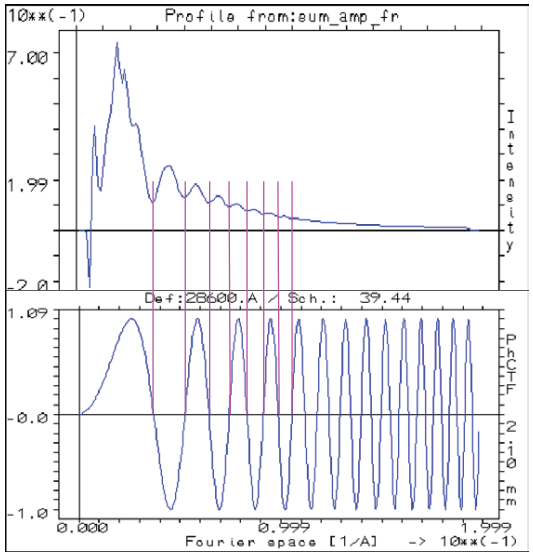

Acceleration VOLTAGE	:	200 kV
CHROMATIC aberration	:	None
SPHERICAL aberration	:	2.1 mm
FOCAL length of objective	:	1.6 mm
APERTURE	:	50.0 micrometer
DEFOCUS values	:	28600.00 A
PIXEL size in curve	:	2.52 A

Alignment: How to assess it

- Clarity of averaged image
- Resemblance to raw data
- Improvement of correlation coefficients with successive iterations
- Low ***variance*** inside molecule projection
- Similar features after classification

Variance

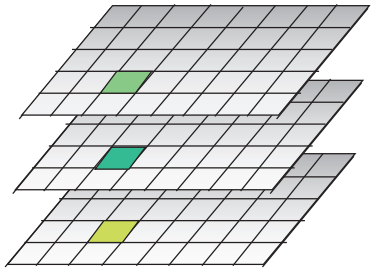

For a stack of aligned images, the variance can be calculated for each pixel, to give a map of variations between the images in the data set. This can help to assess the reliability of features seen on the average image, and can reveal if images of different structures are mixed up in the same data set.

The variance is determined for each pixel as the difference between the pixel value in a given image and the average value of that pixel in all the images. This difference is squared and the sum of these squares is calculated for all the images in the stack.

$$\text{Variance} = [1/(N-1)] \sum_{i,j} [P_i(r_j) - P_{av}(r_j)]^2$$

where $P_i(r_j)$ is the value of pixel j in image i and $P_{av}(r_j)$ is the average value of pixel j in all the images, for a set of N images.

Average and variance of homogeneous and mixed data sets

Set of views with same orientation

Mixture of side views - different orientations around 7-fold (vertical) axis

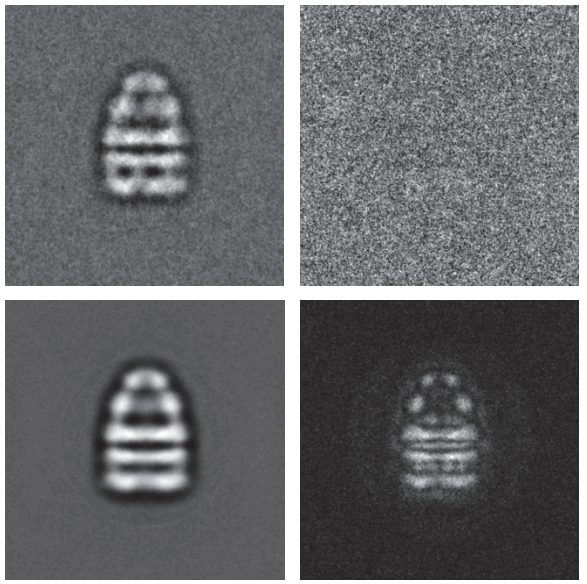

average variance

Current issues in alignment and classification

- **Projection matching** by **cross correlation**: the conventional method is to simply assign the match according to the highest score, which is often not correct, due to noise or model limitations. **Maximum likelihood/Bayesian** methods, as in Relion and Frealign, include noise models and assign multiple matches with different weights.
- Projection matching can be done with class averages or single images, in real or Fourier space
- **Classification** to sort out heterogeneity: e.g. supervised classification (such as ribosome ± factors), separation by multivariate statistical analysis in 2D or 3D, 3D variance calculation by bootstrapping, multiparticle refinement in 3D
- **Model bias** – the starting model must be appropriately filtered to remove features that are not known to be represented in the data:

Einstein from noise – alignment of random noise to an image

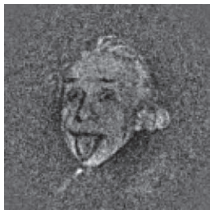

References

Faruqi, A.R. & McMullan, G. (2011). Electron detectors for electron microscopy. Quart. Rev. Biophys **44**, 357-390.

Henderson, R. (1995). The potential and limitations of neutrons, electrons and X-rays for atomic resolution microscopy of unstained biological molecules. Quart. Rev. Biophys. **28**, 171-193.

McMullan, G., Chen, S., Henderson, R.,Faruqi, A. R. , Detective quantum efficiency of electron area detectors in electron microscopy. *Ultramicroscopy* **109**, (2009) 1126-1143.

Li, X. et al (2013) Electron counting and beam-induced motion correction enable near-atomic-resolution single-particle cryo-EM. Nature Methods 10, 584-590.

Bammes, B. et al (2012) Direct electron detection yields cryo-EM reconstructions at resolutions beyond ¾ Nyquist frequency. J. Struct. Biol. 177, 589-601.

Roseman, A.M. (2004). FindEM - a fast, efficient program for automatic selection of particles from electron micrographs. *J. Struct. Biol.* **145**, 91-99.

Chen, J.Z. & Grigorieff, N. (2007). SIGNATURE : A single-particle selection system for molecular electron microscopy. *J. Struct. Biol.* **157**, 168-173.

Elmlund, D & Elmlund, H (2015) Cryogenic electron microscopy and single-particle analysis. Ann Rev Biochem 84, 499-517.

Bai, X, McMullan, G & Scheres, SHW (2015) How cryo-EM is revolutionizing structural biology. TIBS 40, 49-57.

Cheng, Y (2015) Single-particle cryo-EM at crystallographic resolution. Cell 161, 450-457.